Microbial strain-level population structure and genetic diversity from metagenomes

Duy Tin Truong, Adrian Tett, Edoardo Pasolli, et al.

Genome Res. published online February 6, 2017
Access the most recent version at doi:10.1101/gr.216242.116

Microbial strain-level population structure and genetic diversity from metagenomes

Duy Tin Truong[1], Adrian Tett[1], Edoardo Pasolli[1], Curtis Huttenhower[2,3], Nicola Segata[1]

1 Centre for Integrative Biology, University of Trento, Trento, Italy
2 Biostatistics Department, Harvard School of Public Health, Boston, MA, USA
3 The Broad Institute, Cambridge, MA, USA

Corresponding author: Nicola Segata (nicola.segata@unitn.it)

Abstract

Among the human health conditions linked to microbial communities, phenotypes are often associated with only a subset of strains within causal microbial groups. While it has been critical for decades in microbial physiology to characterize individual strains, this has been challenging when using culture-independent high-throughput metagenomics. We introduce StrainPhlAn, a novel metagenomic strain identification approach, and apply it to characterize the genetic structure of thousands of strains from >125 species in >1,500 gut metagenomes drawn from populations spanning North/South American, European, Asian, and African countries. The method relies on per-sample dominant sequence variant reconstruction within species-specific marker genes. It identified primarily subject-specific strain variants (<5% inter-subject strain sharing), and we determined that a single strain typically dominated each species and was retained over time (for >70% of species). Microbial population structure was correlated in several distinct ways with the geographic structure of the host population. In some cases discrete subspecies (e.g. for *Eubacterium rectale* and *Prevotella copri*) or continuous microbial genetic variations (e.g. for *Faecalibacterium prausnitzii*) were associated with geographically distinct human populations, whereas few strains occurred in multiple unrelated cohorts. We further estimated the genetic variability of gut microbes, with *Bacteroides* species appearing remarkably consistent (0.45% median number of nucleotide variants between strains) whereas *P. copri* was among the most plastic gut colonizers. We thus characterize here the population genetics of previously inaccessible intestinal microbes, providing a comprehensive strain-level genetic overview of the gut microbial diversity.

Introduction

Strain-level variants within microbial species are crucial in determining their functional capacities within the human microbiome, including interaction with host tissues (Bron et al. 2012), modulation of immune homeostasis (Needham et al. 2013), and xenobiotic metabolism (Spanogiannopoulos et al. 2016). Pathogenic potential is also strain-specific in many species, including *Escherichia coli*, which is prevalent in the healthy human gut despite some strains causing life-threatening infections (Bielaszewska et al. 2011; Loman et al. 2013) or mucosal necrosis in premature infants (Ward et al. 2016). Strain-level microbial genomic variation typically consists of single-nucleotide variants (SNVs) as well as acquisition/loss of genomic elements including genes, operons, or plasmids (Tettelin et al. 2005). While these genomic features can be accurately characterized in microbial isolates, they have been difficult to study using culture-independent approaches, despite thousands of human-associated metagenomes being available. Translational applications of the human microbiome will require analysis of each community's microbial strain population, ideally in high-throughput from culture-independent sequencing.

Advances in metagenome bioinformatics over the last decade have refined the resolution of microbial community taxonomic profiling from the phylum to the species, but it is still difficult to characterize microbes in communities at the strain level. Metagenomic assembly (Nagarajan and Pop 2013) provides one solution and has been successful in identifying strains of uncharacterized species (Narasingarao et al. 2012; Brown et al. 2015). However, compared to assembling single isolates, metagenomic assembly is computationally challenging, both in efficiency and methodologically in addressing fragmentary contigs, binning, and avoiding chimeric assemblies that combine multiple related strains. To improve metagenomic assembly, extensions that co-assemble multiple metagenomes are also available (Alneberg et al. 2014; Imelfort et al. 2014), but accurate assemblies can require time-consuming manual curation (Sharon et al. 2013; Raveh-Sadka et al. 2015) and it is difficult to generalize the approach to large sets of metagenomes and low abundance microbes.

For microbial communities such as the human microbiome supported by sufficient isolate reference sequences, it is alternatively possible to map the reads of a metagenome against reference genomes and obtain a survey of the single nucleotide variant (SNV) patterns across samples (Schloissnig et al. 2013). Recent signature-based approaches based on marker genes (Franzosa et al. 2015; Luo et al. 2015; Truong et al. 2015) or pan-genes (Scholz et al. 2016) are also able to identify and track strains across samples, but they do not typically allow comprehensive strain cataloging among metagenomes or the reconstruction of microbial phylogenetic relationships in a manner comparable to studies of isolate genomes. As such, it has remained difficult or, in many cases, impossible to profile strains from metagenomes and compare them across a large set of microbiome samples with the same level of resolution attainable by isolate comparative genomics.

In this work, we present StrainPhlAn, a novel method and implementation to profile microbial strains from metagenomes at a resolution comparable with that of isolate sequencing and apply it to thousands of gut samples spanning multiple host populations. The method is based on reconstructing consensus sequence variants within species-specific marker genes and using them to estimate strain-level phylogenies. StrainPhlAn allowed us to process >7 TB of sequencing data from the largest available metagenomic investigations (Qin et al. 2010; Qin et al. 2012; The Human Microbiome Consortium 2012; Karlsson et al. 2013; Le Chatelier et al. 2013; Nielsen et al. 2014; Zeller et al. 2014; Obregon-Tito et al. 2015; Rampelli et al. 2015), yielding large-scale strain-level phylogenies that are used to study the population genomics, biogeography, genetic diversity, and strain retention for 125 intestinal species most of which are sparsely represented in current culture-based investigations.

Results

Enabling strain-level meta-analytic epidemiology of microbial communities and the human microbiome

We developed a novel computational approach to study the strain-level genetics of microbes directly from metagenomic samples and to infer the phylogenetic structure of species across samples. Strains are profiled in each sample by reconstructing a sufficient subset of their genomes for variant calling, which provides a nucleotide-level consensus sequence for each strain. This is carried out by mapping metagenomic reads against species-specific marker sequences (up to 200 per species from a total set of ~1M markers) that are broadly conserved within each species and do not have substantial sequence similarity with genomic regions in other species (Truong et al. 2015). This approach allows strain-specific consensus sequence identifications from as few as a single reference genome (see Methods and Supplemental Fig. S1), and we have verified that variants in these marker genes are representative of whole-genome variability (Supplemental Fig. S2 and S3). The reconstructed strain-specific consensus is independent from the sequence of the marker used as a backbone for the mapping, and can be used for standard phylogenetic analysis (typically multiple sequence alignment (Maiden et al. 1998) followed by phylogenetic reconstruction (Stamatakis 2014)). They can also be used to infer the population structure of strains directly from sets of metagenomes, similarly to the analysis of isolate genomes using shared (core) genes for phylogenetic, population biology, and comparative genomics (Budroni et al. 2011; Segata et al. 2013; Page et al. 2015).

Prevotella copri is a key example of a human commensal for which strain-level comparative genomics from metagenomes is particularly important, since only one cultured isolate reference genome is currently available (Hayashi et al. 2007). It is a frequent colonizer of the human gut (Qin et al. 2010; The Human Microbiome Consortium 2012) that, unusually, occurs abundantly (Arumugam et al. 2011) in only a fraction of the population (from 10% to 25% (Koren et al. 2013)) and has been strongly associated with the onset of rheumatoid arthritis (Scher et al. 2013; Zhang et al. 2015). It is also difficult to culture *ex vivo*, leading to very limited phenotypic and genotypic characterization (Hayashi et al. 2007). By applying StrainPhlAn on *P. copri* directly from gut metagenomes (Fig. 1), we can provide the first characterization of its population genomics in three complementary ways.

First, StrainPhlAn provides a strain-level phylogeny of each analyzed species (in this instance, *P. copri*) from the concatenated alignment of the markers (Fig. 1B-C). When metagenomes are accompanied by phenotypic, environmental, or other metadata annotations, these can be tested for significant association relatively to the population genomic structure of *P. copri* within one or more sub-clades of the phylogeny (Fig. 1D). Finally, the population structure can be visualized by ordination to further identify substructures (e.g. subspecies) in the genetic diversity of the strains (Fig. 1E). Strain-specific consensus sequences from available reference genomes (again, notably only one for *P. copri*) can be included in any of these analyses to compare culture-based genomic information with that extracted from the metagenomes.

Even using this limited set of samples, one can already identify several key new features of *P. copri* population biology. Essentially identical strains are carried in the two longitudinal samples from the same subject (Fig. 1D) and a diverged subspecies clade is also carried near-exclusively within the Chinese population, which is one of roughly four subspecies-level clades of related strains. Even with the reduced set of samples shown here for illustration (see Fig. 4C for the complete analysis), this analysis highlights the use of StrainPhlAn for population genomics of phenotype-relevant microbial community members who are recalcitrant to culture based approaches.

StrainPhlAn achieves per-nucleotide error rates below 0.1%

We first validated the method's precision at the per-nucleotide level using two metagenomes from the HMP mock community (The Human Microbiome Consortium 2012) comprising 21 known organisms (see Methods). This resulted in an error rate (fraction of incorrect nucleotides) below 0.05% overall (Supplementary Table S1). This performance was confirmed on 36 synthetic datasets containing multiple

strains from the same species (see Methods) in which we achieved even lower error rates (<0.03%) for species with coverage >2x (Supplemental Fig. S4), and when considering 36 additional semi-synthetic data comprising gut metagenomes spiked with *in silico* strain-specific reads (<0.2% error rate, Supplemental Fig. S4). When compared to other recent strain-level metagenomic profilers, StrainPhlAn achieved substantially better results than MIDAS (Nayfach et al. 2016) and ConStrains (Luo et al. 2015), based on per-nucleotide and overall strain-tracking accuracies, respectively (Supplemental Tables S1-S5 and Supplemental Figs. S5-S6). In this evaluation, StrainPhlAn was the only method to achieve a resolution in culture-independent strain reconstruction that is comparable with that of isolate genome analysis which is necessary for accurate phylogenetic reconstruction (Supplemental Figs. S5-S6).

We further validated the accuracy of strain identification *in vivo* by using previously sequenced stool samples (Nielsen et al. 2014) from subjects sampled after the intake of a known commercial probiotic bacteria, specifically *Bifidobacterium animalis subsp. lactis* (strain *CNCM I-2494*). In the original work (Nielsen et al. 2014), reconstruction of the *B. animalis* strain was performed by merging together 19 metagenomes from subjects challenged with the probiotic and analyzing the pooled reads. Importantly, this is only possible in cases when it is known *a priori* that the same strain will appear in multiple samples, so the method does not generalize well to most microbes and samples. In contrast, StrainPhlAn allows the analysis of any strain with sufficient sequencing depth per sample, and here we targeted the 7 samples in which the markers of the *B. animalis* species recruited at least 2x coverage. Comparison of our inferred strain consensus profiles to the reference genome achieved <0.01% single nucleotide errors, which is two orders of magnitude lower than the average nucleotide variation (1.3%) between strains from isolate sequencing in the *B. animalis* species and again one or more orders of magnitude lower than the error rate produced by MIDAS (Supplemental Table S6). The phylogeny built by StrainPhlAn using these sequences further placed the *B. animalis* found in these samples among the cluster of reference genomes for this probiotic organism that has been sequenced and assembled several times independently (Supplemental Figs. S7-S8, and Supplemental Table S7). Our approach is also computationally efficient; this example on real gut metagenomes required ~20 minutes per sample and can be further accelerated by parallelization or distributed computing (see Methods), making it appropriate for hundreds of species spanning thousands of metagenomes.

Integrated strain-level population genomics using >1,500 human gut metagenomes

We next applied StrainPhlAn to a set of 1,590 gut metagenomes from adult subjects retrieved from 9 public datasets (Table 1) that we pre-processed using uniform quality control criteria (see Methods) as in (Pasolli et al. 2016). The resulting population spanned all continents except Australia and Antarctica, with curated common metadata including country of origin, health or disease state, age, and BMI (other metadata was either not provided or not common among datasets). It is important to consider that for strain-level population epidemiology, batch effects due to differences in sample collection, storage, DNA extraction, or library preparation are known to affect quantitative profiling, but they are unlikely to influence strain consensus sequence reconstruction from markers. All further analyses below are thus performed on this large set of metagenomes that is diverse in its geographical location, human population of origin, and microbial genetic structure.

We note that, despite a large body of work on strain-level phenotypic characterization and genetic comparisons from microbial isolates, a clear definition of the concept of “strain” is still lacking (Dijkshoorn et al. 2000; Konstantinidis et al. 2006). Genomes differing by just one or a few nucleotides could be defined as different strains, but such limited genetic differences may not result in any phenotypic changes (e.g. synonymous mutations) and would lead to the differentiation of strains in just a few microbial generations. Defining a broader genetic variation threshold can be effective in specific investigations, which is the approach taken by Operational Taxonomic Unit (OTU) definitions in amplicon profiling (Hamady and Knight 2009). However, such hard-limited sequence identity thresholds may be an oversimplification, as they are difficult to set universally and are both locus- and organism-specific. Phylogenetic modelling overcomes the need of defining hard cutoffs for strain or other clade boundaries, and we use this approach to estimate strain relatedness. However, when checking for strain identity is necessary, it is possible to set the threshold considering the intra-individual similarity of retained strains as compared to intra-individual strain heterogeneity.

Single strains dominate most species in the gut microbiome

Analysis of microbial population structures was previously only possible using relatively laborious sequencing of isolate collections; here, we perform high-throughput strain-level profiling directly from a large set of metagenomes spanning multiple geographical locations. In contrast to the 73 prevalent species present in >50% of our >1,500 samples, only ten human-associated species can comparably take advantage of more than 750 sequenced isolates for comparative genetics, and of these only *E. coli* is typically found in the gut. Moreover, sequencing isolates relies on cultivability, whereas our method can investigate members of the human microbiome (or other microbial communities) with fewer biases and no cultivation efforts.

StrainPhlAn reconstructs each species' most abundant strain per sample, and it can assess whether non-dominant strains are present by identifying single nucleotide polymorphisms. We thus first validated the assumption that reconstructing each species' most abundant strain per sample captures most strain-level diversity by assessing how frequently multiple strains per species are detectable in this sample set. In the human gut, most species were represented by a single dominant strain as they show less than 0.1% of nucleotides on the species specific markers that are polymorphic. At this conservative threshold, for 35.7% of cases, no evidence of multiple strains was found at the given depth of sequencing (avg. 5.8 Gnt / sample). Moreover, when the presence of more than one strain was detected, a single strain accounted for at least 80% of each species in another 44.4% of cases. This was determined by identifying, for all samples and markers, the polymorphic and non-polymorphic sites (accounting for sequencing errors, see Methods) and by further estimating the allelic frequency of the dominant variant in polymorphic sites. In order to filter out potentially overestimated frequencies for the cases in which an allele is shared by more than one non-dominant strain of a species in the sample, we consider the median of the frequencies of the dominant allele across polymorphic sites as the frequency of the dominant strain relative to the non-dominant ones. The large majority (>97.8%) of marker nucleotides were not polymorphic at all (Fig. 2A), whereas the remaining nucleotides were largely dominated by a single variant.

Considering all cases in which a species is found in a sample (species-sample combinations), multiple strains were detectable in 14,698 cases (64.3% of species-sample combinations), but it was still rare to find two or more strains at comparable abundance (Fig. 2B). The dominant consensus sequence was less than twice as abundant as all others combined in only 5% of multi-strain cases (Fig. 2B) and in half of the cases, one strain dominated the others by at least 7-to-1 or more. Importantly, all these considerations are independent from the abundance of the species in the samples (Supplemental Fig. S10). When multiple strains were detectable, the fraction of samples in which they were detected varied considerably among species. *Butyrivibrio crossotus*, for example, did not show evidence of strain mixtures in 75% of the 156 samples in which it was detected, whereas more than one strain of *Faecalibacterium prausnitzii* were present in 100% of its 1,052 samples (Fig. 2C). Even in these mixed species, a single strain typically dominated: the main strain of *P. copri* reached on average 86% relative abundance within the species, and similarly for *Butyrivibrio crossotus* (91%), *Faecalibacterium prausnitzii* (78%), *Bacteroides uniformis* (87%), *Bacteroides vulgatus* (91%), and *Ruminococcus bromii* (87%, full list of species in Table S3).

Our analysis suggests that the ecology of multiple closely related strains in the human gut is characterized by the quantitative dominance of one strain. Given the roughly log-normal distribution of species abundances in microbiomes (Li et al. 2012) and the consequent long tail of low-abundance species, non-dominant strains of a species are likely close to or below the limit of detection at typical sequencing depths. Even in an idealized case, a strain making up 5% of a species that itself represents 5% of the overall community, for example, requires a sequencing depth of approximately 2 Gnt to be detected reliably; any strains or species less abundant than this will not be detectable in a typical gut metagenome. Modeling these low-abundance, non-dominant strains would thus largely result in low-quality phylogenetic information and would weaken the advantage of using species-specific marker genes. At the same time, this property makes it very accurate to rely on the frequency of the dominant allele because potential alleles shared by non-dominant strains can have only a minimal impact on the dominant-allele frequency. In our cross-sectional population genomic analysis, we thus focus on the

dominant strain of each detected species, and StrainPhlAn also labels as potentially noisy the rare cases in which two strains from the same species are present at comparable abundances (see Methods).

Gut microbial stability and uniqueness are explained by subject-specific strain retention

With StrainPhlAn, we were able to explain previously observed community-level gut microbiome stability and individuality (Schloissnig et al. 2013; Franzosa et al. 2015) through a mechanism of within-subject strain retention. This parallels the assessment of within-subject strain retention that has been carried out previously for targeted pathogen isolates (Covacci et al. 1999; Nowrouzian et al. 2005; Bidmos et al. 2011). We estimated retention of strains in the gut microbiome by looking at multiple samples from the same participants available from the HMP (The Human Microbiome Consortium 2012) in the absence of disease, and from MetaHIT (Qin et al. 2010; Nielsen et al. 2014), which includes 66 longitudinally sampled patients with inflammatory bowel disease (IBD). To this end, we defined our measure of genetic distance between strains as the length-normalized rate of single nucleotide variants (SNVs) between the full set of markers considered in each species.

We found that, when looking at the same species in two samples from the same individual, the dominant strain of that species was exactly the same in 69% of the longitudinally sampled subjects in MetaHIT and 79% in those from the HMP (Fig. 3) with a percentage of 3.4% and 10.4% of strains that are lost or replaced, on average, each month in the two datasets (Supplemental Fig. S11). The fraction of shared species along longitudinal time points was lower (62.2% in the HMP and 61.1% in MetaHIT), suggesting that detectable species composition is slightly more dynamic than long-term strain retention. This could be explained, for example, by the hypothesis that species are rarely displaced by closely-related competitors, or that when a strain of a species varies in abundance below the limit of detection, it may still be detected later as the same strain. These results help to explain why a strain-level signature of a subject's microbiome is constant in time, particularly in the absence of perturbations from the environment or disease (Franzosa et al. 2015).

In contrast with intra-subject strain retention, strains were rarely shared among individuals: we found evidence of the same strain shared between multiple individuals colonized by a common species in only 3.67% of cases (Fig. 3). A larger fraction of the population shared the same species (35.31% species in common, on average, between two different individuals). Shared geography did not increase the fraction of strains shared by different subjects, as it did not differ significantly within Europe (3.62%) versus worldwide (3.67%). Strains were slightly more commonly shared in the American samples of the HMP (5.13%), but species were less likely to be shared within the HMP (36.0%) as compared to MetaHIT (40.5%). Both of these properties might vary on a less coarse geographical scale, however, and the population enrolled in the HMP was healthy as compared to MetaHIT's longitudinally sampled IBD patients, perhaps leading to greater strain diversity in the latter. Altogether, our analysis highlights the substantial longitudinal strain retention within the same microbial community and the relatively low proportion of strains shared between multiple individuals.

Strain-level microbial genetics strongly correlate with geographically separated host populations

The evolution of specific host-associated microbes is closely linked to factors such as host migrations and transmission mechanisms (vertical, horizontal, environmental); for example, *Helicobacter pylori* is largely vertically transmitted (Delahay and Rugge 2012), and as a result its population genetics is closely linked to the ancestry and geography of its human hosts (Covacci et al. 1999; Suzuki et al. 2012). In this multi-continent meta-analysis, StrainPhlAn permitted the population structure of dominant strains of all species above the limit of detection to be determined in high-throughput. This enabled us to assess, first, which species comprised strains forming a continuum within the overall species diversity, versus those with discrete clusters of strains forming sub-species clades (SCs). The former may be reflective of primarily horizontal transmission between hosts enabling freer gene flow, whereas the latter may reflect sub-speciation due to primarily vertical transmission. In either case, the resulting microbial population structure can be further categorized as randomly or nonrandomly assorted geographically and with respect to host populations.

For *Faecalibacterium prausnitzii* (Sokol et al. 2008; Miquel et al. 2015) 802 distinct strains were detectable in the analyzed samples (Fig. 4A), with only six subjects harboring a strain relatively close (3% SNV rate) to one of the three current isolate genomes. Its genetics were continuously variable and correlated with geography (Fig. 4A); intriguingly, a well-defined subtree of the phylogeny is uniquely composed of strains from the only two non-Westernized populations in this meta-analysis (Peru and Tanzania). *P. copri* showed, conversely, a more discrete population structure, but the resulting SCs were likewise geographically distinct (Fig. 4C). Few strains of *F. prausnitzii* were detected in multiple subjects (13 cases with less than 1% SNV rate), calling out the degree to which this immune-relevant species is under-characterized by current isolate sequencing, which has likewise been confirmed by the few isolates' microbial physiology studies available for this species (Lopez-Siles et al. 2012).

Like *P. copri*, *Eubacterium rectale* strains occurred in distinct SCs forming three genetically distinct groups **(**Fig. 4B-C). *E. rectale*'s discrete population structure was also confirmed by analysis of the strains' gene repertoires (Scholz et al. 2016), further strengthening the finding that this species has three distinct subspecies. Interestingly, one of these was specific to the Chinese population, with 71 of its 74 strains derived from the two Chinese sample sets (Qin et al. 2012; Qin et al. 2014). These two studies were independent and carried out using different protocols and commercial kits for sample collection and DNA extraction and therefore this shows how strain level analysis is not sensitive to the biases in the same way as quantitative analyses. Likewise, few Chinese samples carried *E. rectale* strains from the other two SCs (1 of the 82 strains in one cluster, 20 of the 383 strains in the second).

Other strong geographical associations included the three main SCs of *Bacteroides coprocola* (Supplemental Fig. S12) with Spain (72% prevalence in a 68-strain cluster) and China (80% prevalence in a 49-strain cluster), and the structure of *Ruminococcus bromii* (Supplemental Fig. S13). The striking biogeographical patterns of *Eubacterium* species (Supplemental Figs. S14-S16), and especially of *Eubacterium eligens* (a large Chinese sub-species), *Eubacterium hallii* (Spain), and *Eubacterium siraeum* (Denmark and USA) also suggest that this genus may be particularly prone to population-specific selective pressures. SCs were detected for all prevalent microbial species and, within SCs, strains have very limited genetic diversity (well below 0.1% SNV rate with only very few exception, Supplemental Fig. S17); as expected, inter-SC sequence divergence was instead at least on order of magnitude larger (Supplemental Fig. S17). Like population-specific human genetic alleles, it appears crucial to consider these microbial population structures in future studies of the gut microbiome and its association with host conditions.

Sets of related strains associate with geography even in otherwise cosmopolitan species

Even in species lacking strong, geographically-discrete SCs, groups of related strains often evidenced significant geographic assortment. The ten most prevalent species were present in a comparable fraction of subjects in all cohorts and countries, but single phylogenetic subtrees (of at least 5 strains) were frequently geographically-specific (Fig. 5A). *Bacteroides uniformis* (59% overall prevalence) evidenced China-, Spain- and US-specific subtrees among the 11 largest groups (Fig. 5A). Other species have subtrees completely associated with subjects from Denmark (e.g. *Alistipes putredinis*, and partially *E. rectale* and *Bacteroides dorei*), Spain (all the 10 most prevalent species), Peru (*F. prausnitzii* and *Ruminococcus bromii*), France (*Bacteroides vulgatus*), and again China and US for which the number and size of SCs is influenced by the higher number of subjects available for such nations. These country-specific SCs might reflect selection by host genetics or population history, but the tight co-clustering of strains of *Butyrivibrio crossotus* (Supplemental Fig. S20) and *F. prausnitzii* (Fig. 4A) in the only two cohorts of non-Westernized population (from Peru (Obregon-Tito et al. 2015) and Tanzania (Rampelli et al. 2015)) suggests a potentially dominant role of environmental factors such as diet.

Other SCs comprised instead groups of strains with very little genetic diversity (<0.1% of the total species diversity, see Methods) carried by subjects from different continents. For example, SC66 of *Bacteroides caccae* (Supplemental Fig. S25) includes 59 strains with a median of 0.0169% intra-SC SNV rate from the American (24 subjects), Spanish (7 subjects), Chinese (3 subjects), Danish (3 subjects), and French (4 subjects) populations. Their intra-SC SNV rate is much smaller than the minimum (0.045%) and median (0.344%) diversity of SC66 strains compared to other strains in *B. caccae*. Other SCs within this species were likewise shared across populations (e.g. SC61 or SC71), but *B. caccae* also included

country-specific clades such as SC41 (12 Chinese strains), SC60 (6 Spanish strains), and SC35 (5 Danish strains). *Bacteroides eggerthii* also showed similarly genetically-related SCs that were geographically diverse (Fig. 5B). The genetic consistency of *B. eggerthii* SCs is striking: for the three largest SCs (SC0, SC6, SC7), the intra-SC median genetic diversities (0.026%, 0.014%, and 0.012% respectively) were much smaller than the minimum (0.37%, 0.067%, 0.16%) and median genetic distances (0.50%, 0.46%, 0.46%) between the SCs and the other strains. The set of broadly distributed SCs (see Supplemental Figs. S26-S41 for additional examples) thus likely represents key intestinal subspecies that may be important to further characterize by targeted experiments and isolation.

Genetic diversity of strains in the same species varies significantly for different microbes

It is difficult to define microbial species systematically and to capture each species' diversity appropriately with reference isolates (Achtman and Wagner 2008; Cordero and Polz 2014); for example, *Streptococcus pneumoniae* universal markers differ by up to 5.0% nucleotide identity across 49 strains, compared to only 1.2% among 15 *Streptococcus mitis* strains (Fraser et al. 2009). StrainPhlAn and the large metagenomic dataset we analyzed allowed the assessment of all 125 microbial species' genetic diversities simultaneously as they occurred in a broad population of human guts, regardless of whether an extensive set of reference genomes were available.

For each species containing at least 4 strains, we calculated pairwise genetic distances between strains in the same species. The least variable organism was *B. animalis* (0.018% SNV rate), with markers closely matching those of the commercially available probiotic strain. Given this organism's low prevalence and its identity with the sequence of the commercial strain, it is likely that its presence in the human gut typically results from recent probiotic consumption. The most common intestinal genus, *Bacteroides*, comprises species that are generally genetically consistent (Fig. 6A), with diversity indexes as low as 0.36%, 0.37%, and 0.38% for *B. caccae*, *B. intestinalis*, and *B. massiliensis*, respectively. Other *Bacteroides* species are slightly more diverse (*B. coprocola* 0.73%, *B. coprophilus* 0.75%, *B. stercoris* 0.96%) but are still less genetically variable than other prevalent gut microbes including *Prevotella* species (*P. copri* 2.44%), *F. prausnitzii* (2.94%), *Lactobacillus* (*L. reuteri* 2.74%), *Eubacterium* (*E. siraeum* 1.85%), and some *Ruminococci* (*R. bromii* 1.41%). *Bifidobacteria*, *Parabacteroides*, and *Alistipes* all showed genetic variability in line with that of *Bacteroides*, and all their species have genetic diversities consistent within the corresponding genus (full set of diversity indexes in Supplemental Table S8).

This analysis also revealed many prevalent and/or abundant human gut microbes for which there is a paucity of reference (draft) genomes. Particularly for anaerobic species, we observed genetic diversities between strains more than tenfold larger than what was previously available (Fig. 6B). These included *Faecalibacterium*, *Roseburia intestinalis*, *E. rectale*, *E. siraeum*, and several *Bacteroides* (*B. massiliensis*, *B. ovatus*, *B. salyersiae*, *B. uniformis*, *B. vulgatus*) and *Bifidobacteria* (*B. adolescentis*, *B. bifidum*, *B. pseudocatenulatum*), and they constituted, on average, 63% (s.d. 18%) of the gut microbiome. In contrast, some species that are more conveniently cultured showed a higher diversity than what we sampled from the gut (e.g. *Enterococcus faecium*, *Enterococcus faecalis, Bacteroides fragilis* and some *Clostridia*). This may occur since pathogenic strains (which are arguably more likely to be isolated) are unlikely to be found in healthy conditions or in diseases not associated with single pathogens. Other species with reduced diversity in the gut microbiome included those that are also used for commercial fermentation (bifidobacteria, lactobacilli, *Lactococcus lactis*, *B. fragilis*) and organisms that are more typically found in other environments (e.g. *Lactobacillus saliviarius* and *Streptococcus thermophilus* that are characteristic of the oral microbiome) or non-adult guts (e.g. *Bifidobacterium breve* and *Bifidobacterium dentium* enriched in infants). Overall, the genetic diversity we uncovered here for many common colonizers of the human gut suggests that strain-specificity is a crucial component of host and microbial phenotype that has, using previous methods, been difficult to analyze directly.

Discussion

Here, we have developed a new computational method that enables strain-resolved microbial studies directly from metagenomes, and applied it to characterize the population structure of the human gut microbiome across the globe by combining cohorts totaling >1,500 samples. This approach enables strain-level comparative genetics even for microbes not easily amenable to cultivation, including those

constituting a large portion of the typical human microbiome. The method exploits the concept of species-specific marker genes (Segata et al. 2012) that are used as genetic proxies of species to efficiently profile strains within species from metagenomes. By comparing the consensus sequences of such markers across samples, StrainPhlAn reconstructs both phylogenetic and ecological relationships between strains populating distinct microbial communities. The method proved superior to other available methods and can accurately reconstruct strain-level phylogenies as evaluated on a number of semi-synthetic and real spike-in samples, although assembly- or pangenome-based methods (Sharon et al. 2013; Alneberg et al. 2014; Raveh-Sadka et al. 2015; Scholz et al. 2016) are still required to identify strain-specific gene repertoires. In this study specifically, we phylogenetically profiled thousands of strains from 125 under-characterized intestinal species.

One of the key biological observations of this study is that only one strain typically dominates each species in the human gut, and retention of this individualized dominant strain over time helps to explain the previously reported stability of the gut microbiome (Schloissnig et al. 2013; Franzosa et al. 2015). Strains from the same species in different subjects were generally genetically distinct and associated with host population structure at multiple levels, with different adaptive histories that shaped different species. Even in microbial species defined taxonomically to span roughly the same degree of phylogenetic divergence, some comprised large, discretely differentiated subspecies clades (e.g. *E. rectale*, *P. copri*) while others displayed a genetic continuum with smaller geography-specific subclades (e.g. subclades of *F. prausnitzii* or cosmopolitan strains of *B. eggerthii*). Both of these genetic strategies are in contrast to the tighter genetic control and generally reduced diversity often seen in pathogens, for example the very low divergence rates of *Mycobacterium tuberculosis* (Ford et al. 2011) or infectious (as opposed to more benign) strains of *Streptococcus pneumoniae* (Kilian et al. 2008) or *Staphylococcus aureus* (Holden et al. 2013).

More broadly, the ability to profile strains directly from metagenomes is a key step towards a systems-level understanding of how members of the human microbiome interact with host physiology. Epidemiology and comparative genomics of pathogen populations from isolates has clearly associated specific strains and geography-specific lineages with enhanced virulence potential (Covacci et al. 1999; Suzuki et al. 2012). It will be similarly crucial to associate the presence of strains or subclades of microbial species with immune or chronic disease phenotypes even in the absence of acute infection. The same types of approaches can also start to unravel how members of the microbiome without overt phenotypes are transmitted among hosts, e.g. in vertical mother-to-infant transmission (Milani et al. 2015; Asnicar et al. 2017) or horizontal orofecal routes (Parsonnet et al. 1999). This is of particular interest in the context of interventions such as probiotics or fecal microbiome transplants, in which strain tracking is necessary to identify successful receipt or engraftment of the intended microbes (Li et al. 2016).

Culture-independent strain identification and tracking will also support increasingly high-throughput analyses in microbial ecology. Our finding that a single strain usually dominates per species in the human gut suggests fine-grained microbial competition that might be modifiable by pharmaceutical, nutritional, or environmental interventions. We have investigated only the human gut environment here, making it possible that this is a property specific to that or other host-associated environments, and it would be of interest to test the same hypothesis in other microbial communities. The species-specific genetic structures we characterized also imply multiple evolutionary strategies by which individual microbes adapt and incorporate into communities. Discrete subspecies may result from vertical convergent evolution with low horizontal gene flow, whereas species without distinct subclade boundaries (e.g. *F. prausnitzii*) are likely the results of more plastic genomes subject to recombination and lateral gene exchange. This has been described in a few specific cases such as oral neisseriae (Donati et al. 2016), but the relative ease with which thousands of metagenomes can now be obtained compared to isolate (Browne et al. 2016) or single-cell (Gawad et al. 2016) sequencing makes StrainPhlAn profiling of large metagenomes collections a key tool for the understanding of the ecology of the human gut and other microbial communities.

Methods

StrainPhlAn infers the strain-level phylogenetic structure of microbial species across metagenomic samples by reconstructing the consensus sequences of the dominant strain for each detected species in a sample and then comparing the consensus sequences in different samples (Fig. S1). The method takes as input metagenomic samples and a species-specific marker set, in this case using the markers calculated for MetaPhlAn2 (Truong et al. 2015). Metagenomic reads are aligned to the marker genes and a consensus sequence is built for each marker. Then, for each species, the consensus sequences in each sample are aligned and concatenated. The concatenated alignments are then used to produce phylogenetic trees using the maximum-likelihood reconstruction principle. Downstream visualization and ordination plots provided directly in the StrainPhlAn package include ordination and sub-phylogeny analysis and allow cross-referencing the inferred phylogenies with available sample metadata. The user can also choose to include in the phylogenies available references genomes that are useful for providing context for the strains found in the metagenomic samples.

The StrainPhlAn algorithm

To execute the overall workflow described above, metagenomic reads in each sample are first mapped against the species specific MetaPlAn2 markers using Bowtie2 (Langmead and Salzberg 2012). The resulting alignments are processed with BAMtools (Li et al. 2009) to estimate the consensus sequence of each detected species-specific marker. This is performed using a simple majority rule to infer each nucleotide of the markers. Strain-specific markers can also be extracted from available reference genomes (using Blastn (Altschul et al. 1990)) to include them in the downstream analysis, if chosen by the user.

A number of post-processing operations are then applied in order to perform multiple sequence alignment on high-quality consensus sequences and concatenate them in consistent larger alignments for each species. Specifically, reconstructed markers with a percentage of ambiguous bases (resulting from low-confidence majority rule application or lack of coverage for some regions of the maker) greater than 20% are discarded. Consensus sequences are then trimmed by removing the first and last *n* bases (parameter "–marker_strip_length", default 50), because the terminal positions are affected by lower coverages due to the limitations in mapping reads against truncated sequences. Strain profiling in a sample, by default, is only provided for species where the number of reconstructed markers exceeds 80% of the total number of markers available for that species in the MetaPhlAn2 database (this threshold can be defined by the user with the "–marker_in_clade" parameter). After these steps, the reconstructed markers from each metagenomic sample, and if chosen by the user those from the reference genomes, are aligned using MUSCLE (Edgar 2004).

For each marker, the resulting multiple sequence alignments are then processed to remove poorly covered regions. First, both ends of the alignment are trimmed until the fraction of gaps in each position is less than 20% (parameter "–-gap_in_trailing_col", default 20%). Secondly, regions across the remaining alignment that are present in only a small fraction of samples, below 30%, are also removed (parameter "–gap_in_internal_col", default 30%). Thirdly, if the number of the alignment columns with at least one ambiguous nucleotide (i.e. "Ns") is less than 80% of the total number of columns (parameter "–N_col", default 80%), the columns with ambiguous nucleotides are removed. After these steps, the remaining ambiguous nucleotides ("Ns") in the alignment are replaced with gaps to meet the requirements of the phylogeny reconstruction software.

Next, the processed multiple sequence alignments, for each of the target species, are concatenated. Comparing the concatenated alignment across samples, if the number of long-gap positions (i.e. at least three continuous gap positions) in the concatenated alignment is smaller than 80% of the total length (parameter "–-long_gap_percentage", default 80%), we remove the corresponding columns. Finally, strains that have gaps in more than 20% of the alignment (parameter "–-gap_in_sample", default 20%) are also removed from the alignment. The edited concatenated alignment is then processed with the maximum-likelihood phylogenetic inference software RAXML (Ott et al. 2007) to produce the phylogenetic trees. Custom scripts are available in our package to build the ordination plots and the heatmaps of genetic-distance matrices. The metadata information is then added to these plots for supporting the discovery of new associations with the population structure of the species (using the script add_metadata.py).

StrainPhlAn required an average of 20 minutes on a single CPU for profiling all strains in a single high-depth metagenomic sample (averages computed across all the >1,590 samples analyzed that comprise, on average, ~5.8Gb). This is in addition to the pre-requisite MetaPhlAn2 step (111 minutes per CPU). In our analysis, a total of 10 hours (single CPU) was required to reconstruct the strain-level phylogeny (including sequence merging, multiple-sequence alignment, and maximum-likelihood based phylogenetic inference) for each of the 125 species analyzed across the entire 1,590 gut metagenomic dataset.

Polymorphic site identification

To identify and study the presence of multiple strains from the same species in a single sample, we investigated the reads-to-markers mapping and sought evidence of polymorphic sites on the alignments suggestive of multiple alleles. To this end, we defined, for each position s on the alignment of the reads against the N_s as the total number of reads covering it and T_s as the number of reads supporting the dominant (i.e. most abundant) allele. Given the sequencing error rate E, we reject the non-polymorphic null hypothesis if the probability that the number $N_s - T_s$ of reads coming from the non-dominant allele is less than α=0.05. This is estimated with $P_{X\sim B(N_s,1-E)}(X \leq T_s)$ where $B(N_s, 1-E)$ is the probability mass function of a binomial distribution with N_s trials and the successful rate $1-E$. We set the error rate E to 0.01 (i.e. 1%) for Illumina sequencing. Failing to reject the null hypothesis reflects the absence of alternative alleles or inability of distinguishing between low-coverage potential alternative alleles and sequencing noise. To further minimize the impact of noise, we remove the bases with quality below 30 before applying the statistical test. To summarize the polymorphic site probabilities at the species level (thus marking the probabilities of multiple sites and markers), we define a polymorphic species as a species having a polymorphic rate greater than $\mu_{\text{polymorphic rate}} + \sigma_{\text{polymorphic rate}}$ where $\mu_{\text{polymorphic rate}}$ and $\sigma_{\text{polymorphic\_rate}}$ are the median and standard deviation of the polymorphic site across samples, respectively.

Retention rate and subclade computation

For each species, we computed the rate of single nucleotide variants (SNV) between the dominant strains in different samples. The intra-individual SNV rate was calculate for the HMP and MetaHIT datasets as they are the only considered datasets with multiple samples from the same subjects. The SNV rates for each species was normalized by the median of the inter-everyone comparisons for that species. The resulting distribution is bimodal and represents the distribution of variations between same strains in different samples (values close to zero) and different strains (values centered in the normalized median, i.e. 1.0). For identifying the bimodal distributions, we fitted a two-component Gaussian mixture model and separated the dominant component in the ranges $[-\infty, \mu + 3\sigma]$ or $[\mu - 3\sigma, +\infty]$.

Country-specific subtrees for Figs. S9-S20 are computed as the largest subtrees with at least 80% of samples coming from a single country. For identifying the clusters in the principal coordinate plots (Fig. 4), we used the SpectralClustering algorithm implemented in Scikit-learn (Pedregosa et al. 2011) applied on the first two principal coordinates. Subclades for Fig. 5B and Figs.S21-S37 are the largest subtrees in each phylogeny with the largest intra-SNVs rate smaller than 0.1%. In addition, a subclade must have strains from at least two subjects or contain at least one reference genome and one strain in a sample.

Data Collection and Preprocessing

In total, 1,590 publically available gut metagenomics samples comprising nine human-associated datasets were considered in this work (Table 1). Of these studies, seven were associated with human disease and two from healthy cohorts. The cohort datasets spanned geographic locations from all continents (except Australia and Antarctica) and two included non-Westernized populations from Peru and Tanzania. All datasets are cross-sectional, with the exception of two cohorts (MetaHIT and HMP) which included longitudinal sampling of the same individuals over a period of 163 s.d. 125 days and 219 s.d. 69 days respectively. When the same sequenced samples were originally included in more than one study (i.e. some samples from the Obesity dataset (Le Chatelier et al. 2013) are present also in the MetaHIT dataset (Nielsen et al. 2014)) we considered them only once in our combined dataset.

All samples were preprocessed by the standard HMP quality control procedure (The Human Microbiome Consortium 2012) and reads shorter than the thresholds reported in Table 1 were removed. Taxonomic profiling to identify which microbial species are present and at what abundance in each sample, was performed with MetaPhlAn2 (Truong et al. 2015).

Method validation and evaluation

For validation, StrainPhlAn was applied to a combination of synthetic and semi-synthetic datasets. StrainPhlAn was first tested on two HMP Mock samples (The Human Microbiome Consortium 2010) containing strains from 21 known reference genomes where their abundances were either staggered or evenly distributed. StrainPhlAn reconstructed the strains for the 11 species with sufficient coverage (Table S1). Except for *Staphylococcus aureus* and *Clostridium beijerinckii* (whose genomes are discordant also based on metagenomic assembly, see Table S1), our method can reconstruct the other species strains with the SNV rates <0.0001.

In addition, we also validated StrainPhlAn on 36 synthetic datasets of 4 species (*Bacteroides dorei, Bacteroides fragilis, Bacteroides ovatus, Bifidobacterium longum*). For each species, we generated synthetic data by sampling reads from its genomes with an Illumina-based error model (McElroy et al. 2012) with coverages ranging from 2x to 10x using custom scripts available at https://bitbucket.org/CibioCM/synmetap/overview. These synthetic samples were then also added to real HMP stool metagenomes (in which the four synthetic species was absent) to create 36 additional semi-synthetic samples. StrainPhlAn was applied on both synthetic and semi-synthetic samples, and the accuracy was evaluated by detecting the number of SNV of the reconstructed markers compared to the original reference genomes. The evaluation was repeated at increasing coverages of the target strains as reported in Fig. S2. An additional validation was performed by reconstructing strain markers from synthetic metagenomes and including them in the phylogeny built with the reference genomes (Figs. S3-S4). On the combined phylogeny, the accuracy of the reconstruction can be evaluated by measuring the phylogenetic distance between the reconstructed strains and the corresponding reference genome (Figs. S3-S4). ConStrains (Luo et al. 2015) was applied on the same data (Figs. S3-S4). For the validation on real samples (Fig. S5, Table S2), we used nineteen metagenomes in the MetaHIT (Nielsen et al. 2014) dataset from subjects that consumed a fermented milk product containing the previously sequenced *Bifidobacterium animalis subsp. lactis CNCM I-2494*.

Acknowledgments

We thank the Human Microbiome Project Consortium and all the volunteers and researchers involved in the large-scale metagenomic efforts considered in this study. This work was supported in part by NIH grants R01HG005969 and U54DE023798, NSF grant DBI-1053486 and Army Research Office grant W911NF-11-1-0473 to C.H., Fondazione Caritro grant Rif. Int.2014.0325 to A.T., European Union H2020 Marie-curie grant (707345) to E.P., and was supported by a European Union FP7 Marie-Curie grant (PCIG13-618833), MIUR grant FIR RBFR13EWWI, Fondazione Caritro grant Rif. Int.2013.0239, Leo Pharma Research Foundation, and Terme di Comano grants to N.S.

Software Availability

StrainPhlAn (version 1.0) is implemented in Python within the MetaPhlAn2 package (version 2.5.0) and is available with source code, manual, tutorials and a support user group at http://segatalab.cibio.unitn.it/tools/strainphlan and in the updated MetaPhlAn2 repository at http://segatalab.cibio.unitn.it/tools/metaphlan2/. The code and necessary supporting databases are maintained in a Bitbucket repository at https://bitbucket.org/biobakery/metaphlan2. A snapshot of the implementation used in this work are also available as Supplementary Code, without however the large database files that are maintained at https://bitbucket.org/biobakery/metaphlan2.

Tables

Table 1. Sizes and characteristics of the nine large-scale metagenomic datasets used in this study.

Dataset	Number of samples	Number of reads (x 10^9)	Minimum read length	Diseases or Conditions	Country
HMP (The Human Microbiome Consortium 2012)	196	20.70	90	Healthy (196)	USA (196)
WT2D (Karlsson et al. 2013)	145	4.53	90	Impaired glucose tolerance (49) Type 2 diabetes (53) Healthy (43)	Sweden (130), other EU countries (15)
Cirrhosis (Qin et al. 2014)	232	11.91	90	Liver cirrhosis (118) Healthy (114)	China (232)
T2D (Qin et al. 2012)	290	12.36	90	Type 2 diabetes (137) Healthy (153)	China (290)
CRC (Zeller et al. 2014)	134	7.78	90	Colorectal cancer (48) Large adenoma (13) Small adenoma (26) Healthy (47)	France (156)
Obesity (Le Chatelier et al. 2013)	115	10.35	75	Underweight (41) Obese (70) Healthy (4)	Denmark (115)
PAG (Obregon-Tito et al. 2015)	58	2.73	70	Underweight (1) Overweight (10) Obese (5) Healthy (42)	Peru (36), USA (22)
MetaHIT (Nielsen et al. 2014)	382	20.84	70	Crohn disease (21) Healthy relatively (47) Ulcerative colitis (127) Healthy (187)	Denmark (163) Spain (219)
AIG (Rampelli et al. 2015)	38	0.85	90	Healthy (38)	Tanzania (27) Italy (11)
Total	1590	92.05	70	Diseased (871) Healthy (719)	Four continents

Figure captions

Fig. 1: StrainPhlAn for strain identification and tracking in shotgun metagenomes and its application to *Prevotella copri* in the human gut. StrainPhlAn provides a method to identify strains from shotgun metagenomes and provides tracking, comparative, and phylogenetic analyses across samples. Here, we illustrate results using *Prevotella copri* as an example species in a demonstration subset of this study's human gut metagenomes. (**A**) In this overview of the method, for each species for which strains are to be analyzed across a metagenome collection, sample-specific and strain-specific markers are constructed by mapping reads against the MetaPhlAn2 (Truong et al. 2015) database of species-specific reference sequences. (**B**) In each sample, species are identified and quantified if sufficient coverage for the species markers is detected. Here, 100 samples with sufficiently abundant *P. copri* are shown (seven other abundant species are also displayed). (**C**) The pre-selected species-specific markers are concatenated, aligned, and variants identified using the consensus sequence of mapped metagenomic reads. (**D**) From the resulting set of the most abundant strains per sample, a phylogenetic tree can be built. This allows, for example, retained or minimally divergent strains within a particular environment (e.g. human host) to be easily identified when they appear within the same subtrees. (**E**) Strains or subtrees can also be statistically associated with sample metadata (e.g. human or environmental phenotypes), and (**F**) each species' genetic diversity and divergence can be easily visualized as an ordination comparable to those used for isolate or human population genetics.

Fig. 2. Most species are dominated by a single strain in the human gut. (**A**) Distribution of dominant allele frequency for all nucleotide positions in concatenated species-specific markers across all analyzed

samples (>482M total nucleotides). (**B**) Distribution of the dominant allele frequency for polymorphic positions. We report the median frequencies for each species/sample pair. (**C**) Distribution of non-polymorphic site prevalence in samples for the ten most prevalent gut bacterial species (full set of species in Supplemental Fig. S9). The fraction of non-polymorphic sites varies from sample to sample and from species to species. In parenthesis we quantify the percentage of strains with >99.9% of non-polymorphic sites.

Fig. 3. Most strains are retained over time within the human gut, but few strains are carried by multiple subjects. The distribution of the all-versus-all normalized genetic distance between strains is reported for increasingly large metagenome collections (only MetaHIT, only the HMP, or all 1,590 samples). For MetaHIT and the HMP, we also computed the intra-subject distances (temporal separation between samplings averaging 163 s.d. 125 days and 219 s.d. 69 days, respectively) normalized based on the median of the all-versus-all comparisons.

Fig. 4. Population genetic structure of three common intestinal species and its association with sampling geography. Strain population structures for three representative human gut species, reported both as phylogenies built on the concatenated alignments of each species-specific reconstructed marker set (bottom). In order to highlight the presence of discrete clusters of related strains, we also report the genetic distances measured on the alignments as principal coordinate ordinations (above). We report the population structure of (**A**) *Faecalibacterium prausnitzii*, (**B**) *Eubacterium rectale* and (**C**) *Prevotella copri*. Results for additional species are reported in Supplemental Figs. S12-S16, S18-S24.

Fig. 5. Associations between sub-species clades and geographical location in the ten most prevalent gut species and *Bacteroides eggerthii*. (**A**) For each of the ten most prevalent species and *Bacteroides eggerthii* in this sample set, we show the prevalence of each country in the 11 largest subtrees, ordered by size. Subtrees containing reference isolate genomes are marked with a black border. Information regarding subtrees for all species is available as Supplemental Figs. S42-S44**.** (**B**) Example phylogenetic tree of *Bacteroides eggerthii* with the identified subclades.

Fig. 6. Overall species diversity evaluated across intestinal samples and compared with the diversity available from reference genomes. (**A**) For the 112 species with concatenated marker length greater than 10,000 nt, we built a phylogenetic tree using PhyloPhlAn (Segata et al. 2013) and GraPhlAn (Asnicar et al. 2015) and report here their median SNV rate computed on all pairwise comparisons in this sample set. The median SNV of each genus is reported in parenthesis in the legend. Species diversity ranges between 0.018% (*B. animalis*) to 3.9% (*Phascolarctobacterium succinatutens*) and are partially correlated with phylogeny (*Bacteroides, Parabacteroides, Bifidobacterium*, and *Alistipes* species show consistently lower diversity than *Prevotella*, *Lactobacillus*, and *Streptococcus* species). No significant correlation between diversity and total prevalence or average abundance was observed (Supplemental Fig. S45). Detailed information for each species is reported in Supplemental Table S9. (**B**) Fraction of total branch length spanned by strains sequenced as isolate reference genomes versus branch length spanned by strains from metagenomes. This figure includes species with at least 10 samples, 3 reference genomes, and concatenated marker length greater than 10,000 nt. The complete set of species are provided in Supplemental Fig. S46.

References

Achtman M, Wagner M. 2008. Microbial diversity and the genetic nature of microbial species. *Nature reviews Microbiology* **6**(6): 431-440.

Alneberg J, Bjarnason BS, de Bruijn I, Schirmer M, Quick J, Ijaz UZ, Lahti L, Loman NJ, Andersson AF, Quince C. 2014. Binning metagenomic contigs by coverage and composition. *Nat Methods* **11**(11): 1144-1146.

Altschul SF, Gish W, Miller W, Myers EW, Lipman DJ. 1990. Basic local alignment search tool. *Journal of molecular biology* **215**(3): 403-410.

Arumugam M, Raes J, Pelletier E, Le Paslier D, Yamada T, Mende DR, Fernandes GR, Tap J, Bruls T, Batto JM et al. 2011. Enterotypes of the human gut microbiome. *Nature* **473**(7346): 174-180.

Asnicar F, Manara S, Zolfo M, Truong DT, Scholz M, Armanini F, Ferrretti P, Gorfer V, Pedrotti A, Tett A. 2017. Studying vertical microbiome transmission from mothers to infants by strain-level metagenomic profiling. *mSystems* **2**(1): e00164-00116.

Asnicar F, Weingart G, Tickle TL, Huttenhower C, Segata N. 2015. Compact graphical representation of phylogenetic data and metadata with GraPhlAn. *PeerJ* **3**: e1029.

Bidmos FA, Neal KR, Oldfield NJ, Turner DP, Ala'Aldeen DA, Bayliss CD. 2011. Persistence, replacement, and rapid clonal expansion of meningococcal carriage isolates in a 2008 university student cohort. *Journal of clinical microbiology* **49**(2): 506-512.

Bielaszewska M, Mellmann A, Zhang W, Kock R, Fruth A, Bauwens A, Peters G, Karch H. 2011. Characterisation of the Escherichia coli strain associated with an outbreak of haemolytic uraemic syndrome in Germany, 2011: a microbiological study. *The Lancet Infectious diseases* **11**(9): 671-676.

Bron PA, van Baarlen P, Kleerebezem M. 2012. Emerging molecular insights into the interaction between probiotics and the host intestinal mucosa. *Nature reviews Microbiology* **10**(1): 66-78.

Brown CT, Hug LA, Thomas BC, Sharon I, Castelle CJ, Singh A, Wilkins MJ, Wrighton KC, Williams KH, Banfield JF. 2015. Unusual biology across a group comprising more than 15% of domain Bacteria. *Nature*.

Browne HP, Forster SC, Anonye BO, Kumar N, Neville BA, Stares MD, Goulding D, Lawley TD. 2016. Culturing of 'unculturable' human microbiota reveals novel taxa and extensive sporulation. *Nature* **533**(7604): 543-546.

Budroni S, Siena E, Dunning Hotopp JC, Seib KL, Serruto D, Nofroni C, Comanducci M, Riley DR, Daugherty SC, Angiuoli SV et al. 2011. Neisseria meningitidis is structured in clades associated with restriction modification systems that modulate homologous recombination. *Proceedings of the National Academy of Sciences of the United States of America* **108**(11): 4494-4499.

Cordero OX, Polz MF. 2014. Explaining microbial genomic diversity in light of evolutionary ecology. *Nature reviews Microbiology* **12**(4): 263-273.

Covacci A, Telford JL, Del Giudice G, Parsonnet J, Rappuoli R. 1999. Helicobacter pylori virulence and genetic geography. *Science (New York, NY)* **284**(5418): 1328-1333.

Delahay RM, Rugge M. 2012. Pathogenesis of Helicobacter pylori infection. *Helicobacter* **17 Suppl 1**: 9-15.

Dijkshoorn L, Ursing BM, Ursing JB. 2000. Strain, clone and species: comments on three basic concepts of bacteriology. *Journal of medical microbiology* **49**(5): 397-401.

Donati C, Zolfo M, Albanese D, Truong DT, Asnicar F, Iebba V, Cavalieri D, Jousson O, De Filippo C, Huttenhower C. 2016. Uncovering oral Neisseria tropism and persistence using metagenomic sequencing. *Nature Microbiology*: 16070.

Edgar RC. 2004. MUSCLE: multiple sequence alignment with high accuracy and high throughput. *Nucleic acids research* **32**(5): 1792-1797.

Ford CB, Lin PL, Chase MR, Shah RR, Iartchouk O, Galagan J, Mohaideen N, Ioerger TR, Sacchettini JC, Lipsitch M et al. 2011. Use of whole genome sequencing to estimate the mutation rate of Mycobacterium tuberculosis during latent infection. *Nature genetics* **43**(5): 482-486.

Franzosa EA, Huang K, Meadow JF, Gevers D, Lemon KP, Bohannan BJ, Huttenhower C. 2015. Identifying personal microbiomes using metagenomic codes. *Proceedings of the National Academy of Sciences of the United States of America* **112**(22): E2930-2938.

Fraser C, Alm EJ, Polz MF, Spratt BG, Hanage WP. 2009. The bacterial species challenge: making sense of genetic and ecological diversity. *Science (New York, NY)* **323**(5915): 741-746.

Gawad C, Koh W, Quake SR. 2016. Single-cell genome sequencing: current state of the science. *Nature reviews Genetics* **17**(3): 175-188.

Hamady M, Knight R. 2009. Microbial community profiling for human microbiome projects: Tools, techniques, and challenges. *Genome Res* **19**(7): 1141-1152.

Hayashi H, Shibata K, Sakamoto M, Tomita S, Benno Y. 2007. Prevotella copri sp. nov. and Prevotella stercorea sp. nov., isolated from human faeces. *International journal of systematic and evolutionary microbiology* **57**(Pt 5): 941-946.

Holden MT, Hsu LY, Kurt K, Weinert LA, Mather AE, Harris SR, Strommenger B, Layer F, Witte W, de Lencastre H et al. 2013. A genomic portrait of the emergence, evolution, and global spread of a methicillin-resistant Staphylococcus aureus pandemic. *Genome Res* **23**(4): 653-664.

Imelfort M, Parks D, Woodcroft BJ, Dennis P, Hugenholtz P, Tyson GW. 2014. GroopM: an automated tool for the recovery of population genomes from related metagenomes. *PeerJ* **2**: e603.

Karlsson FH, Tremaroli V, Nookaew I, Bergstrom G, Behre CJ, Fagerberg B, Nielsen J, Backhed F. 2013. Gut metagenome in European women with normal, impaired and diabetic glucose control. *Nature* **498**(7452): 99-103.

Kilian M, Poulsen K, Blomqvist T, Havarstein LS, Bek-Thomsen M, Tettelin H, Sorensen UB. 2008. Evolution of Streptococcus pneumoniae and its close commensal relatives. *PloS one* **3**(7): e2683.

Konstantinidis KT, Ramette A, Tiedje JM. 2006. The bacterial species definition in the genomic era. *Philosophical transactions of the Royal Society of London Series B, Biological sciences* **361**(1475): 1929-1940.

Koren O, Knights D, Gonzalez A, Waldron L, Segata N, Knight R, Huttenhower C, Ley RE. 2013. A guide to enterotypes across the human body: meta-analysis of microbial community structures in human microbiome datasets. *PLoS computational biology* **9**(1): e1002863.

Langmead B, Salzberg SL. 2012. Fast gapped-read alignment with Bowtie 2. *Nature methods* **9**(4): 357-359.

Le Chatelier E, Nielsen T, Qin J, Prifti E, Hildebrand F, Falony G, Almeida M, Arumugam M, Batto JM, Kennedy S et al. 2013. Richness of human gut microbiome correlates with metabolic markers. *Nature* **500**(7464): 541-546.

Li H, Handsaker B, Wysoker A, Fennell T, Ruan J, Homer N, Marth G, Abecasis G, Durbin R. 2009. The sequence alignment/map format and SAMtools. *Bioinformatics* **25**(16): 2078-2079.

Li K, Bihan M, Yooseph S, Methe BA. 2012. Analyses of the microbial diversity across the human microbiome. *PloS one* **7**(6): e32118.

Li SS, Zhu A, Benes V, Costea PI, Hercog R, Hildebrand F, Huerta-Cepas J, Nieuwdorp M, Salojarvi J, Voigt AY et al. 2016. Durable coexistence of donor and recipient strains after fecal microbiota transplantation. *Science (New York, NY)* **352**(6285): 586-589.

Loman NJ, Constantinidou C, Christner M, Rohde H, Chan JZ, Quick J, Weir JC, Quince C, Smith GP, Betley JR et al. 2013. A culture-independent sequence-based metagenomics approach to the investigation of an outbreak of Shiga-toxigenic Escherichia coli O104:H4. *Jama* **309**(14): 1502-1510.

Lopez-Siles M, Khan TM, Duncan SH, Harmsen HJ, Garcia-Gil LJ, Flint HJ. 2012. Cultured representatives of two major phylogroups of human colonic Faecalibacterium prausnitzii can utilize pectin, uronic acids, and host-derived substrates for growth. *Applied and environmental microbiology* **78**(2): 420-428.

Luo C, Knight R, Siljander H, Knip M, Xavier RJ, Gevers D. 2015. ConStrains identifies microbial strains in metagenomic datasets. *Nature biotechnology* **33**(10): 1045-1052.

Maiden MC, Bygraves JA, Feil E, Morelli G, Russell JE, Urwin R, Zhang Q, Zhou J, Zurth K, Caugant DA et al. 1998. Multilocus sequence typing: a portable approach to the identification of clones within populations of pathogenic microorganisms. *Proceedings of the National Academy of Sciences of the United States of America* **95**(6): 3140-3145.

McElroy KE, Luciani F, Thomas T. 2012. GemSIM: general, error-model based simulator of next-generation sequencing data. *BMC genomics* **13**: 74.

Milani C, Mancabelli L, Lugli GA, Duranti S, Turroni F, Ferrario C, Mangifesta M, Viappiani A, Ferretti P, Gorfer V et al. 2015. Exploring Vertical Transmission of Bifidobacteria from Mother to Child. *Applied and environmental microbiology* **81**(20): 7078-7087.

Miquel S, Leclerc M, Martin R, Chain F, Lenoir M, Raguideau S, Hudault S, Bridonneau C, Northen T, Bowen B et al. 2015. Identification of metabolic signatures linked to anti-inflammatory effects of Faecalibacterium prausnitzii. *mBio* **6**(2).

Nagarajan N, Pop M. 2013. Sequence assembly demystified. *Nature reviews Genetics* **14**(3): 157-167.

Narasingarao P, Podell S, Ugalde JA, Brochier-Armanet C, Emerson JB, Brocks JJ, Heidelberg KB, Banfield JF, Allen EE. 2012. De novo metagenomic assembly reveals abundant novel major lineage of Archaea in hypersaline microbial communities. *The ISME journal* **6**(1): 81-93.

Nayfach S, Rodriguez-Mueller B, Garud N, Pollard KS. 2016. An integrated metagenomics pipeline for strain profiling reveals novel patterns of bacterial transmission and biogeography. *Genome Research* **26**(11): 1612-1625.

Needham BD, Carroll SM, Giles DK, Georgiou G, Whiteley M, Trent MS. 2013. Modulating the innate immune response by combinatorial engineering of endotoxin. *Proceedings of the National Academy of Sciences of the United States of America* **110**(4): 1464-1469.

Nielsen HB, Almeida M, Juncker AS, Rasmussen S, Li J, Sunagawa S, Plichta DR, Gautier L, Pedersen AG, Le Chatelier E et al. 2014. Identification and assembly of genomes and genetic elements in complex metagenomic samples without using reference genomes. *Nat Biotechnol* **32**(8): 822-828.

Nowrouzian FL, Wold AE, Adlerberth I. 2005. Escherichia coli strains belonging to phylogenetic group B2 have superior capacity to persist in the intestinal microflora of infants. *The Journal of infectious diseases* **191**(7): 1078-1083.

Obregon-Tito AJ, Tito RY, Metcalf J, Sankaranarayanan K, Clemente JC, Ursell LK, Zech Xu Z, Van Treuren W, Knight R, Gaffney PM et al. 2015. Subsistence strategies in traditional societies distinguish gut microbiomes. *Nature communications* **6**: 6505.

Ott M, Zola J, Stamatakis A, Aluru S. 2007. Large-scale maximum likelihood-based phylogenetic analysis on the IBM BlueGene/L. In *Proceedings of the 2007 ACM/IEEE conference on Supercomputing*, p. 4. ACM.

Page AJ, Cummins CA, Hunt M, Wong VK, Reuter S, Holden MT, Fookes M, Falush D, Keane JA, Parkhill J. 2015. Roary: rapid large-scale prokaryote pan genome analysis. *Bioinformatics* **31**(22): 3691-3693.

Parsonnet J, Shmuely H, Haggerty T. 1999. Fecal and oral shedding of Helicobacter pylori from healthy infected adults. *Jama* **282**(23): 2240-2245.

Pasolli E, Truong DT, Malik F, Waldron L, Segata N. 2016. Machine learning meta-analysis of large metagenomic datasets: tools and biological insights. *PLoS computational biology* **12**(7): e1004977.

Pedregosa F, Varoquaux G, Gramfort A, Michel V, Thirion B, Grisel O, Blondel M, Prettenhofer P, Weiss R, Dubourg V. 2011. Scikit-learn: Machine learning in Python. *The Journal of Machine Learning Research* **12**: 2825-2830.

Qin J, Li R, Raes J, Arumugam M, Burgdorf KS, Manichanh C, Nielsen T, Pons N, Levenez F, Yamada T et al. 2010. A human gut microbial gene catalogue established by metagenomic sequencing. *Nature* **464**(7285): 59-65.

Qin J, Li Y, Cai Z, Li S, Zhu J, Zhang F, Liang S, Zhang W, Guan Y, Shen D et al. 2012. A metagenome-wide association study of gut microbiota in type 2 diabetes. *Nature* **490**(7418): 55-60.

Qin N, Yang F, Li A, Prifti E, Chen Y, Shao L, Guo J, Le Chatelier E, Yao J, Wu L. 2014. Alterations of the human gut microbiome in liver cirrhosis. *Nature*.

Rampelli S, Schnorr Stephanie L, Consolandi C, Turroni S, Severgnini M, Peano C, Brigidi P, Crittenden Alyssa N, Henry Amanda G, Candela M. 2015. Metagenome Sequencing of the Hadza Hunter-Gatherer Gut Microbiota. *Current Biology* **25**(13): 1682-1693.

Raveh-Sadka T, Thomas BC, Singh A, Firek B, Brooks B, Castelle CJ, Sharon I, Baker R, Good M, Morowitz MJ. 2015. Gut bacteria are rarely shared by co-hospitalized premature infants, regardless of necrotizing enterocolitis development. *Elife* **4**: e05477.

Scher JU, Sczesnak A, Longman RS, Segata N, Ubeda C, Bielski C, Rostron T, Cerundolo V, Pamer EG, Abramson SB et al. 2013. Expansion of intestinal Prevotella copri correlates with enhanced susceptibility to arthritis. *Elife* **2**: e01202.

Schloissnig S, Arumugam M, Sunagawa S, Mitreva M, Tap J, Zhu A, Waller A, Mende DR, Kultima JR, Martin J et al. 2013. Genomic variation landscape of the human gut microbiome. *Nature* **493**(7430): 45-50.

Scholz M, Ward DV, Pasolli E, Tolio T, Zolfo M, Asnicar F, Truong DT, Tett A, Morrow AL, Segata N. 2016. Strain-level microbial epidemiology and population genomics from shotgun metagenomics. *Nat Methods*.

Segata N, Bornigen D, Morgan XC, Huttenhower C. 2013. PhyloPhlAn is a new method for improved phylogenetic and taxonomic placement of microbes. *Nature communications* **4**: 2304.

Segata N, Waldron L, Ballarini A, Narasimhan V, Jousson O, Huttenhower C. 2012. Metagenomic microbial community profiling using unique clade-specific marker genes. *Nature methods* **9**(8): 811-814.

Sharon I, Morowitz MJ, Thomas BC, Costello EK, Relman DA, Banfield JF. 2013. Time series community genomics analysis reveals rapid shifts in bacterial species, strains, and phage during infant gut colonization. *Genome research* **23**(1): 111-120.

Sokol H, Pigneur B, Watterlot L, Lakhdari O, Bermudez-Humaran LG, Gratadoux JJ, Blugeon S, Bridonneau C, Furet JP, Corthier G et al. 2008. Faecalibacterium prausnitzii is an anti-inflammatory commensal bacterium identified by gut microbiota analysis of Crohn disease patients. *Proceedings of the National Academy of Sciences of the United States of America* **105**(43): 16731-16736.

Spanogiannopoulos P, Bess EN, Carmody RN, Turnbaugh PJ. 2016. The microbial pharmacists within us: a metagenomic view of xenobiotic metabolism. *Nature reviews Microbiology* **14**(5): 273-287.

Stamatakis A. 2014. RAxML version 8: a tool for phylogenetic analysis and post-analysis of large phylogenies. *Bioinformatics*: btu033.

Suzuki R, Shiota S, Yamaoka Y. 2012. Molecular epidemiology, population genetics, and pathogenic role of Helicobacter pylori. *Infection, genetics and evolution : journal of molecular epidemiology and evolutionary genetics in infectious diseases* **12**(2): 203-213.

Tettelin H, Masignani V, Cieslewicz MJ, Donati C, Medini D, Ward NL, Angiuoli SV, Crabtree J, Jones AL, Durkin AS. 2005. Genome analysis of multiple pathogenic isolates of Streptococcus agalactiae: implications for the microbial "pan-genome". *Proceedings of the National Academy of Sciences of the United States of America* **102**(39): 13950-13955.

The Human Microbiome Consortium. 2010. HMMC - Mock Community 16S & WGS Reads (http://hmpdacc.org/HMMC/).

-. 2012. Structure, function and diversity of the healthy human microbiome. *Nature* **486**(7402): 207-214.

Truong DT, Franzosa EA, Tickle TL, Scholz M, Weingart G, Pasolli E, Tett A, Huttenhower C, Segata N. 2015. MetaPhlAn2 for enhanced metagenomic taxonomic profiling. *Nat Methods* **12**(10): 902-903.

Ward DV, Scholz M, Zolfo M, Taft DH, Schibler KR, Tett A, Segata N, Morrow AL. 2016. Metagenomic Sequencing with Strain-Level Resolution Implicates Uropathogenic E. coli in Necrotizing Enterocolitis and Mortality in Preterm Infants. *Cell reports* **14**(12): 2912-2924.

Zeller G, Tap J, Voigt AY, Sunagawa S, Kultima JR, Costea PI, Amiot A, Bohm J, Brunetti F, Habermann N et al. 2014. Potential of fecal microbiota for early-stage detection of colorectal cancer. *Molecular systems biology* **10**: 766.

Zhang X, Zhang D, Jia H, Feng Q, Wang D, Liang D, Wu X, Li J, Tang L, Li Y et al. 2015. The oral and gut microbiomes are perturbed in rheumatoid arthritis and partly normalized after treatment. *Nature medicine* **21**(8): 895-905.

A

Metagenomic dataset

Sample 1
@read_1
CGAAGATTGCT
+read_1
GGFGGGFGGG
@read_2
CCACCCT
+read_2
GGGGGG
FastQ

Sample 2
@read_1
CGAAGATT
+read_1
GGFGGGFG
@read_2
CCACCCTGAC
+read_2
GGGGGGFGE
FastQ

Reads-to-markers Mapping

Species-specific Markers
@*Prevotella_copri*_marker_1
CATGCAGATATCCATGTTATCATATCATGAG
@*Prevotella_copri*_marker_2
TCACGTGAACCTCACCTAATCCTACTAGCTG
@*Bacteroides_caccae*_marker_1
AGCTTTAATCCTAGGAACCTCTGAGGATTA
@*Bacteroides_caccae*_marker_2
GGAAACCATCACCTCTTAACCAATCAACAT

Marker Identification

Reference genomes
@*Prevotella_copri_genome_1*
CATGCAGATATCCATGTCTCCATAT
@*Bacteroides_caccae*_genome_2
GGAAACCATCACCATCACCCTCTCT

B

Species-level abundance

E. coli
R. bromii
P. stercorea
D. invisus
S. unclassified
B. crossotus
F. prausnitzii
P. copri

Samples

0 10 20 30 40 50 60 70 80

C Strain-level alignment

1 2126 3219 5435 64734

Samples & Reference genomes

[...] [...] [...] [.....]

P. copri marker 1 marker 2 marker 98

Denmark France Spain China
USA Peru Reference genomes

D

the same subject

13 6 10

E

13 6 10

F

PC2

PC1

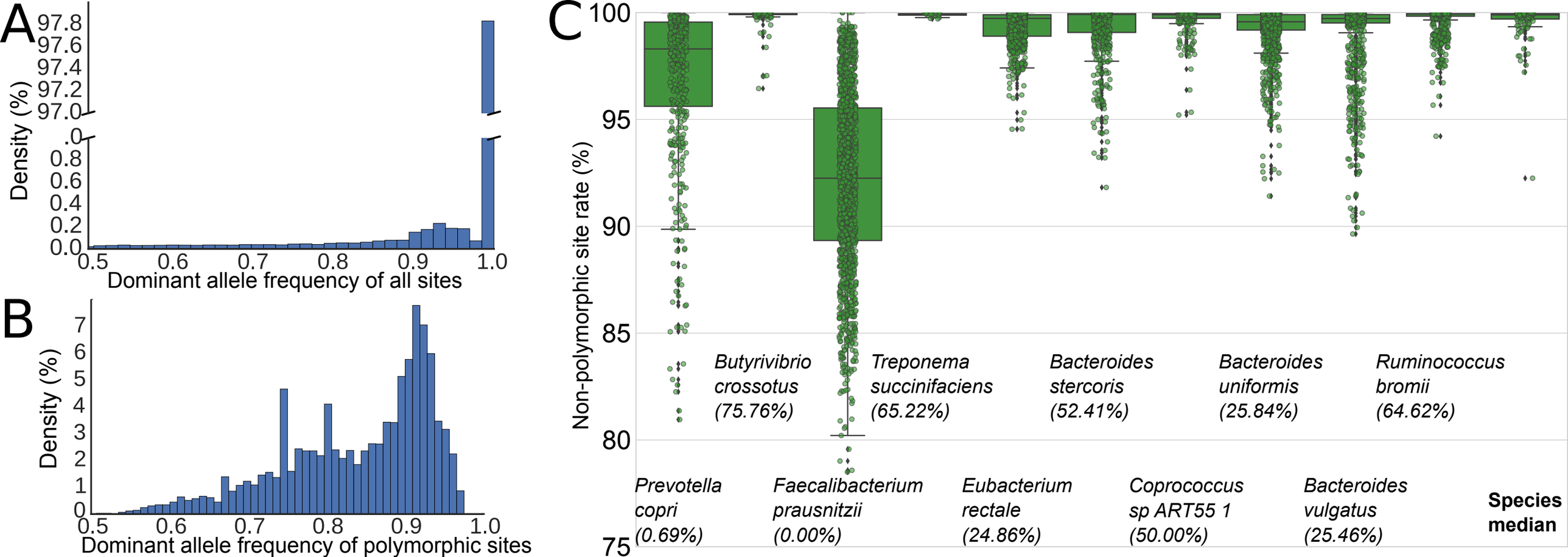
A
97.8
97.6
97.4
97.2
97.0
.0
0.8
0.6
0.4
0.2
0.0
Density (%)
0.5
0.6
0.7
0.8
0.9
1.0
Dominant allele frequency of all sites
B
7
6
5
4
3
2
1
0
Density (%)
0.5
0.6
0.7
0.8
0.9
1.0
Dominant allele frequency of polymorphic sites
C
100
95
90
85
80
75
Non-polymorphic site rate (%)
Butyrivibrio crossotus (75.76%)
Treponema succinifaciens (65.22%)
Bacteroides stercoris (52.41%)
Bacteroides uniformis (25.84%)
Ruminococcus bromii (64.62%)
Prevotella copri (0.69%)
Faecalibacterium prausnitzii (0.00%)
Eubacterium rectale (24.86%)
Coprococcus sp ART55 1 (50.00%)
Bacteroides vulgatus (25.46%)
Species median

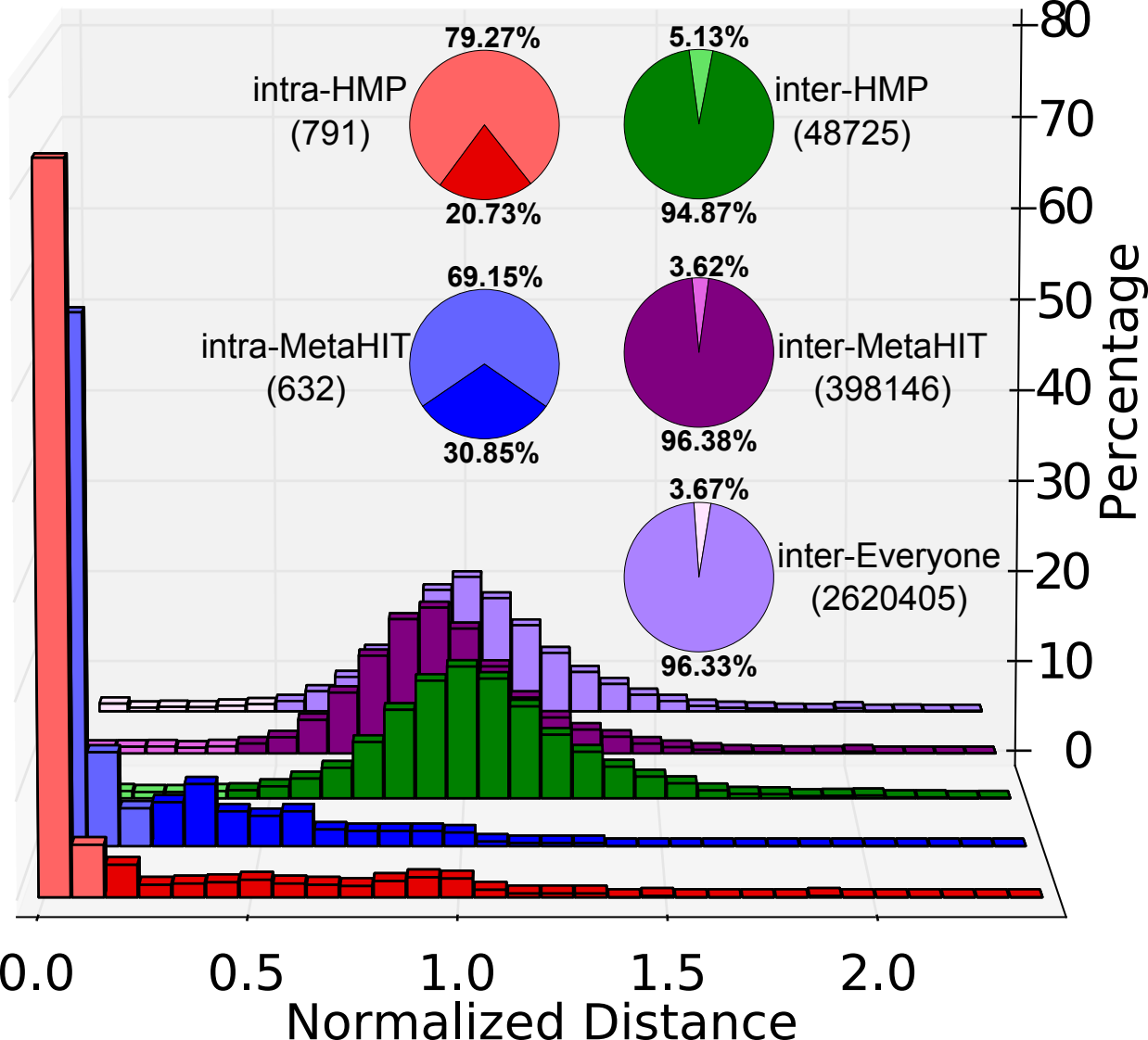
79.27%
intra-HMP
(791)
20.73%
5.13%
inter-HMP
(48725)
94.87%
69.15%
intra-MetaHIT
(632)
30.85%
3.62%
inter-MetaHIT
(398146)
96.38%
3.67%
inter-Everyone
(2620405)
96.33%
80
70
60
50
40
30
20
10
0
Percentage
0.0
0.5
1.0
1.5
2.0
Normalized Distance

A

Faecalibacterium prausnitzii

PC2

PC1

B

Eubacterium rectale

PC2

PC1

C

Prevotella copri

PC2

PC1

China
Spain
Denmark
Tanzania
France
Sweden
Italy
USA
Peru
Reference genomes

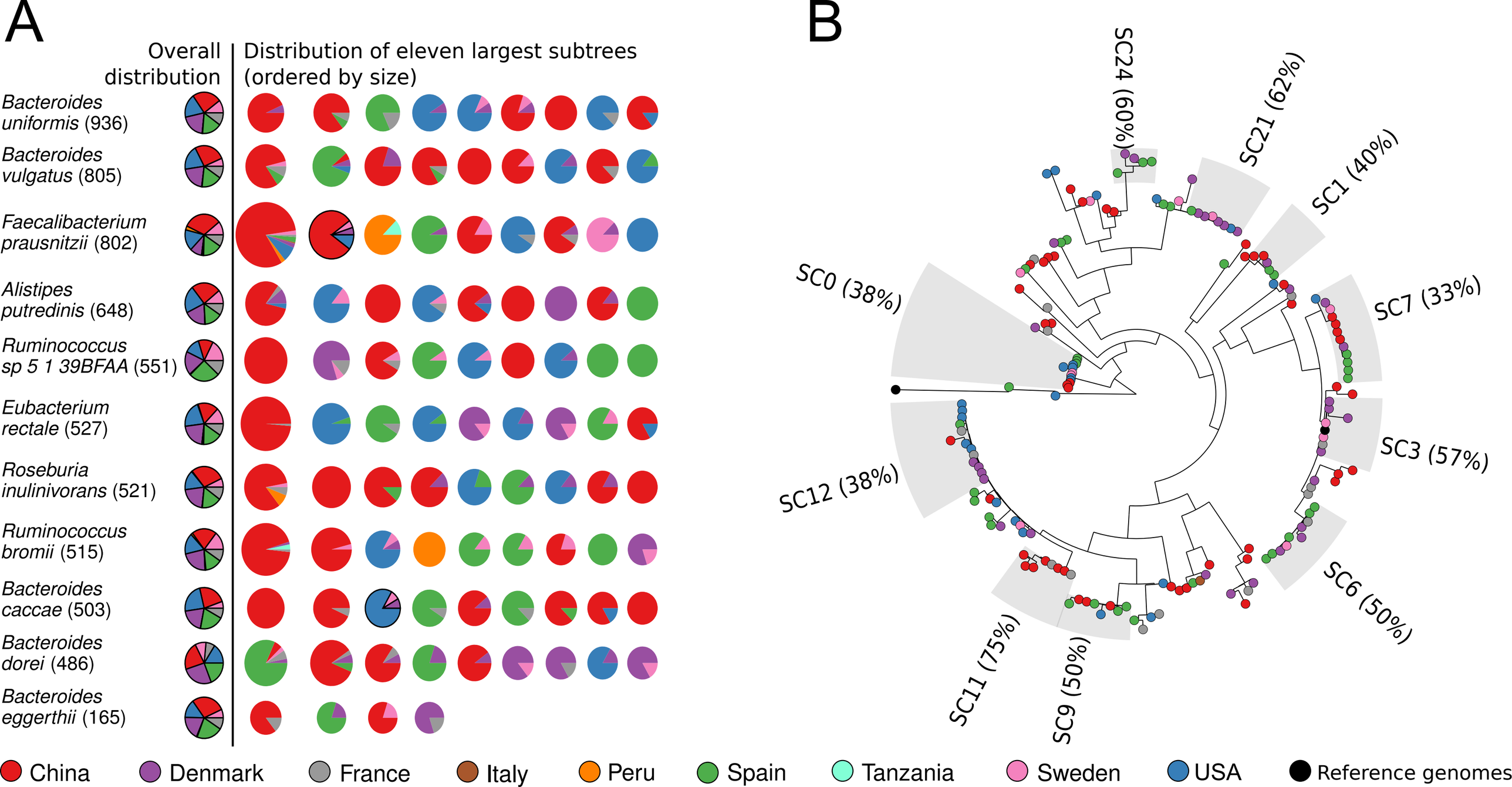
A
Overall distribution
Distribution of eleven largest subtrees (ordered by size)
Bacteroides uniformis (936)
Bacteroides vulgatus (805)
Faecalibacterium prausnitzii (802)
Alistipes putredinis (648)
Ruminococcus sp 5 1 39BFAA (551)
Eubacterium rectale (527)
Roseburia inulinivorans (521)
Ruminococcus bromii (515)
Bacteroides caccae (503)
Bacteroides dorei (486)
Bacteroides eggerthii (165)
B
SC24 (60%)
SC21 (62%)
SC1 (40%)
SC7 (33%)
SC3 (57%)
SC6 (50%)
SC9 (50%)
SC11 (75%)
SC12 (38%)
SC0 (38%)
China
Denmark
France
Italy
Peru
Spain
Tanzania
Sweden
USA
Reference genomes